Synchrotron radiation X-ray for static and dynamic flow visualization of the ultrathin heat pipe

Chun-Hui Wu(吳俊輝)[1], Gung-Chian Yin(殷廣鈐)[2], Chien-Yu Lee(李建佑)[2], Ming-Ying Hsu(徐名瑩)[2], Bo-Yi Chen(陳伯毅)[2], and Ping-Hei Chen(陳炳煇)[1*]

[1] Department of Mechanical Engineering, National Taiwan University, Taipei, 10617, Taiwan
[2] Experimental Technique Group, National Synchrotron Radiation Research Center, Hsinchu 30076, Taiwan.
phchen@ntu.edu.tw

Abstract

This study explored the feasibility of using synchrotron radiation X-ray phase-contrast imaging for the visualization of static liquid distribution and dynamic liquid movement within ultrathin heat pipes. An experimental study of ultrathin heat pipes with a thickness of 0.5 mm was performed with different filling ratios and heating temperatures. For static flow visualization, liquid distribution ratios decreased linearly with the increasing heating temperatures in various ultrathin heat pipes. Liquid distribution was random, and liquid films and droplets could attach on a wall or coalesce with each other during operations. For dynamic flow visualization, water vapors could coalesce with the present liquid film or droplet at any moment when flowing through an adiabatic section. Droplet growth was heterogeneous, and the measured average droplet growth rates increased with the increasing designated heating temperatures.

Keywords - synchrotron radiation X-ray, phase-contrast imaging, flow visualization, ultra-thin heat pipe

Introduction

Although heat pipes have been developed for more than 50 years, mechanisms and theoretical limit estimations have been appropriately established. However, flow field visualization of a heat pipe is still one of the most interesting but difficult topics in engineering. In general, a transparent material (e.g., glass [1] or acrylic [2]) is mounted on a sample as an observation area. Or the complete sample was made by a transparent material [3]. However, the surface properties of transparent materials, such as surface roughness and surface wettability, are considerably different from those of the original metal pipe wall. The flow field and flow behavior are somehow affected.The features of X-ray phase-contrast imaging are suitable for measuring the liquid–vapor interface movement of a working fluid in ultrathin heat pipes. In this study, synchrotron radiation X-ray phase-contrast imaging was employed to directly visualize static liquid distribution and dynamic liquid movement within ultrathin heat pipes. Ultrathin heat pipes with a thickness of 0.5 mm were experimentally examined with different filling ratios and heating temperatures. For an improved understanding of ultrathin heat pipes, an investigation of the liquid movement and liquid distribution is required.

Experimental setup

Fig. 1 shows the schematic of the experimental setup: (a) front view and (b) a photo of ultrathin heat pipes. In this study, three different types of ultrathin heat pipes were measured in this study. The dimensions of these ultrathin heat pipes were identical, that is, 7.7 mm(W) × 77 mm (L) × 0.5 mm (H), and the wall thicknesses were all 0.1 mm. Deionized water was used as the working fluid in various ultrathin heat pipes. The amount of working fluid in type-1, -2, and -3 are 0.025, 0.5, 0.75 g, respectively. Copper wire braids were used in this study as wick structures; had a wire diameter of 0.05 mm. Heat was provided by a ceramic plate heater with a microprocessor controller for temperature control. The thermoelectric (TE) cooler was connected with a power supply at the condenser section of the ultrathin heat pipe for heat removal. The voltage and current of the TE cooler power supply were 2 V and 1 A. No insulation material was used outside the ultrathin heat pipe to prevent X-ray-phase contrast decay. Two sets of thermocouples (K-type) designated for measuring the temperatures of evaporator and condenser sections. A thermometer data logger was used to read data measured using these thermocouples for further analysis.

All experiments were conducted at the BL 12B2 of SPring-8 in Hyogo, Japan. An X-ray beamline with an energy of 30 keV was used in this study. The captured images were then correspondingly stitched based on horizontal and vertical positions. The range of the designated temperature of the heat was 25 ℃–40 ℃. Figure 2 (a) presents the local zoom-in and stitched experimental images for the designated heating temperature of 25 ℃ and cooling temperature of 14 ℃. Figure 2 (b) shows liquid distribution within an ultrathin heat pipe applied with polygon edge detection.

Results and Discussion

Fig. 3 presents the results of liquid distribution ratios at various heating temperatures in various ultrathin heat pipes. For all types of ultrathin heat pipes, the liquid distribution ratios linearly decreased with the increasing heating temperatures. At high heating temperatures, high amounts of liquid were vaporized from the evaporator section and then transported to the condenser section, which resulted in low liquid distribution ratios at high heating temperatures. However, an extreme negative slope corresponds with the limited range of operational temperatures. However, the values of the measured liquid distribution ratios were evidently different. Such observations can primarily be attributed to three factors. First, the observed area was smaller than the observable area, i.e., not all ultrathin heat pipes were observed.

Liquid distribution in the unobserved region was unknown. Second, the liquid could possibly cover a part of copper wires or form liquid bridges between copper wires. Liquid distribution within copper wire braids was not measurable because the phase contrast between the copper wire braids and liquid was low and thus could not be distinguished. Third, because of the fabrication process, the copper wire braids in the ultrathin heat pipes were not perfectly placed in the middle of the chamber. Moreover, the compactness of the copper wire braids in each ultrathin heat pipe varied. The aforementioned three factors engender differences between the liquid distribution ratios and filling ratio in various ultrathin heat pipes.

For dynamic flow visualization experiments, power provided to the TE cooler was 0.1 W to minimize temperature fluctuation for observation during the heating process. The observed area in Fig. 4 was in the middle of the ultrathin heat pipe. The evaporator section was on the right-hand side, and the condenser section was on the left-hand side. The edge profiles of the droplet 5 and liquid film 6 in Figs. 4 were blurry, and the average growth rate for droplet 5 and liquid film 6 was not calculated. Fig. 4 shows liquid movement variation with time in the adiabatic section of the type-3 ultrathin heat pipe at the designated heating temperature of 40 ℃ for (a) t = 0 s, (b) t = 152 s, (c) t = 646 s, and (d) t = 682 s. During the heating process, the size of droplets 1 and 2 had significantly increased with time. Droplet 3 did not initially exist. However, droplet 3 suddenly popped out at t = 152 s. Moreover, with the increasing size of droplet 3, it coalesced with liquid film 6 at t = 646 s. Finally, droplet 4 coalesced with the liquid film 6 at t = 682 s. This phenomenon indicated that the liquid does not only exist in the condenser section or copper wire braids. When the vapor flows through the adiabatic section, it could coalesce with the existent droplet or liquid film. The flatness, surface wettability, cleanness of the inner and outer walls may affect liquid movements. The droplet growth was heterogeneous, and the average droplet growth rates for droplets 1 and 2 in Fig. 5 were 485.5 and 238.7 μm2/s, respectively.

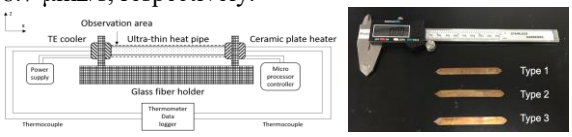

(a) (b)

Figure 1. Schematic of the experimental setup: (a) front view, (b) the photo of the ultrathin heat pipes.

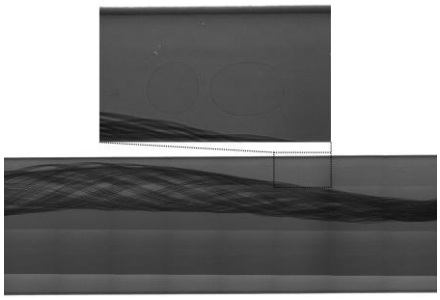

(a)

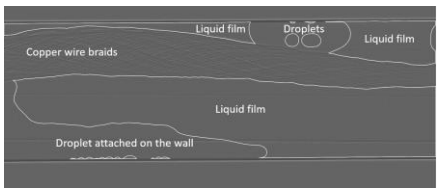

(b)

Figure 2. Image processing procedures (a) local zoom-in and stitched images, (b) applied with polygon edge detection.

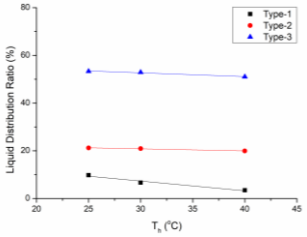

Figure 3. Liquid distribution ratios at various heating temperatures in various ultrathin heat pipes.

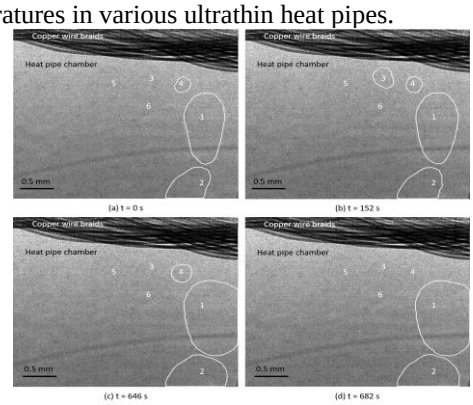

Figure 4. Liquid movement variation with time in the adiabatic section of the type-3 ultrathin heat pipe for a designated heating temperature of 40℃: (a) t = 0 s, (b) t = 152 s, (c) t = 646 s, and (d) t = 682 s.

Acknowledgments

The authors like to thank Yen-Fa Liao, Ph. D. from Taiwan Beamline Office at SPring-8 of NSRRC for experimental assistance in SPring-8, Hyogo, Japan. This work was financially sponsored by the Ministry of Science and Technology, Taiwan, ROC, under grant number 105-2221-E-002-107-MY3.

References

[1] S.-C. Wong, W.-S. Liao, Visualization experiments on flat-plate heat pipes with composite mesh-groove wick at different tilt angles, International Journal of Heat and Mass Transfer, 123 (2018) 839-847.

[2] H. W. Park, S. J. Lee, S. Y. Jung, X-ray imaging analysis on behaviors of boiling bubbles in nanofluids, International Journal of Heat and Mass Transfer, 128 (2019) 443-449.

[3] I. G. Kim, K. M. Kim, Y. S. Jeong, I.C. Bang, Flow visualization and heat transfer performance of annular thermosyphon heat pipe, Applied Thermal Engineering, 125 (2017) 1456-1468.